About the effect of plastic dissipation in heat at the crack tip on the stress intensity factor under cyclic loading

N. Ranc[a], T. Palin-Luc[b,*], P. C. Paris[c], N. Saintier[b]

[a] *Arts et Metiers ParisTech, PIMM, CNRS, 151 Boulevard de l'Hôpital, F-75013 Paris, France*
[b] *Arts et Metiers ParisTech, I2M, CNRS, Universite Bordeaux 1, Esplanade des Arts et Metiers, F-33405 Talence, France*
[c] *Parks College of Engineering, Aviation, and Technology, St. Louis University St. Louis, MO, 63103 USA and visiting professor at Arts et Metiers ParisTech, France*

Abstract

Because of the reverse cyclic plastic zone at the crack tip, there is plastic dissipation in heat at the crack tip under cyclic loading. That creates a heterogeneous temperature field around the crack tip. A thermo-mechanical model is proposed in this paper for evaluating the consequence of this temperature field on the Mode I stress intensity factor. Two cases are studied: (i) the theoretical problem of an infinite plate with a semi-infinite through crack under Mode I cyclic loading, and (ii) a finite specimen with a central through crack. In the first case, the main hypothesis and results are presented from the literature but no heat loss is taken into account. In second case, heat loss by convection is taken into account with a finite element analysis, while an analytical solution exists in the literature for the first case. In both cases, it is assumed that the heat source is located in the reverse cyclic plastic zone. The heat source within the reverse cyclic plastic zone is quantified by experiments on a mild steel under R=0.1. It is shown that the crack tip is under compression due to thermal stresses coming from the heterogeneous temperature field around the crack tip. The effect of this stress field on the stress intensity factor (its maximum, minimum and its range) is calculated. This paper shows that experiments have to be carried out to determine the heat source within the reverse cyclic plastic zone. This is the key parameter to quantify the effect of dissipation at the crack tip on the stress intensity factor.

Keywords: stress intensity factor, plastic dissipation, reverse cyclic plastic zone, thermal stress

*Corresponding author
Email addresses: nicolas.ranc@ensam.eu (N. Ranc), thierry.palin-luc@ensam.eu (T. Palin-Luc), pcparis30@gmail.com (P. C. Paris), nicolas.saintier@ensam.eu (N. Saintier)
URL: http://i2m.u-bordeaux.fr (T. Palin-Luc)

Nomenclature

a	thermal diffusivity
c	crack length
q	heat source per unit length of the crack front
r	radius
r_R	radius of the reverse cyclic plastic zone
t	time
u_r, u_θ, u_z	radial, circumferential and out of plane displacement, respectively
C	heat capacity
E	Young modulus
$K_{I,cyc}$	stress intensity factor in Mode I due to the fatigue cyclic loading
$K_{I,temp}$	stress intensity factor in Mode I due to the temperature gradient
$K_{I,max}$	maximum stress intensity factor in Mode I
$K_{I,min}$	minimum stress intensity factor in Mode I
K_{th}	threshold stress intensity factor in Mode I
Pe	Péclet number
α	linear coefficient of thermal expansion
ε_r, ε_θ, ε_z	radial, circumferential and out of plane strains, respectively
λ	heat conductivity
ρ	density
σ_r, σ_θ, σ_z	radial, circumferential and out of plane normal stresses, respectively
σ_y	yield stress
ν	Poisson ratio
$\mathcal{E}$	dissipated energy per unit length of crack front during one cycle
ϑ	temperature variation field depending on time t and radius r
ΔK_I	range of the Mode I stress intensity factor

1. Introduction

It is known in the literature [1, 2] that during plastic strain a significant part of the plastic energy (around 90% for metals) is converted in heat. During a cyclic loading of a cracked structure, the plasticity is located in the reverse cyclic plastic zone near the crack tip. This phenomenon was first explained by Paris in 1964 [3] and studied later by Rice in 1967 [4]. This effect is now well-known and participates for instance in the explanation of the crack closure phenomenon which was first identified by Elber in 1970 [5]. As was noticed by the authors in 2011 [6], the dissipated energy in the reverse cyclic plastic zone also generates a heterogeneous temperature field which depends on the intensity of the heat source associated with the plasticity and the thermal boundary conditions of the cracked structure. Due to the thermal expansion of the material, the temperature gradient near the crack tip creates thermal stresses which contribute to the stress field in this region.

The main aim of this work is to quantify the effect of the heterogeneous temperature field on the stress intensity factor. The previous paper by the authors [6] was devoted to the theoretical problem of an infinite plate with a semi-infinite through crack without any heat loss. Indeed, there are two significant problems to solve when estimating the thermal stresses: the first one is the quantification of the heat source associated with the plasticity near the crack tip; the second one is to make a good estimation of the boundary conditions of the thermal problem (convection from the surface of the cracked structure, for example). The heat source has to be deduced from experimental temperature field measurement with an inverse numerical method (using finite element analysis). The geometry of a real specimen has to be taken into account together with the convection boundary conditions over all the specimen surfaces.

The present paper is first focused on the theoretical problem of an infinite plate with a semi-infinite through crack under fatigue loading in Mode I (Figure 1). The hypothesis and the main results associated to this problem, solved by the authors in 2011 [6], are recalled to understand the most significant phenomena. Then, the heat source within the reverse cyclic plastic zone is identified from temperature field measurement (with an infrared camera) at the surface of a central cracked specimen. In this case the thermal losses due to convection cannot be neglected like in the previous theoretical problem (infinite plate with a central through crack). A finite element analysis including the thermal losses (convection) allows the authors to compute the temperature field on the specimen, to estimate the thermal stresses due to this heterogeneous temperature field and to quantify their effect on the Mode I stress intensity factor. It is shown that the crack tip is under compressive thermal stresses which reduce the

crack driving force. Finally, some recommendations for further theoretical and experimental investigations are proposed.

2. An infinite plate with a semi-infinite through crack

2.1. The temperature field due to the heat source within the reverse cyclic plastic zone

During crack growth under cyclic loading, the cyclic plastic strains at each cycle are confined within the reverse cyclic plastic zone. A portion of the plastic strain energy is dissipated in heat and generates a temperature variation. Generally, the size of this reverse cyclic plastic zone is very small. In order to determine the temperature field, it is possible to consider the thermal problem associated with the fatigue crack propagation as a line heat source centered in the reverse cyclic plastic zone along the crack tip in an infinitely thick body. Ranc et al. [6] have compared the numerical solution (by finite element analysis) of the thermal problem in the case of a uniform heat source in a cylinder with a radius equal to the radius of the reverse cyclic plastic zone (Figure 1) and the analytical solution of the thermal problem with a line heat source. The temperature variation fields obtained with the line heat source or the uniform heat source hypothesis are very close to eachother outside the reverse cyclic plastic zone: the relative difference is equal to about 0.03%. However, the temperature inside the reverse cyclic plastic zone can be very differently distributed, but this is not the aim of this paper. This study is focused on the effect of the temperature gradient on the stress state outside this plastic zone, in order to calculate the consequences on the stress intensity factor.

The dissipated power per unit length of crack front is assumed to be proportional to the surface area of the reverse cyclic plastic zone and the loading frequency f [7]:

$$q = f\mathcal{E} = f\eta r_R^2, \tag{1}$$

with $\mathcal{E}$ the dissipated energy per unit length of crack front during one cycle, r_R the radius of the reverse cyclic plastic zone and η a material-dependent proportionality factor.

It is well-known in the literature that, both in plane stress and plane strain, the reverse cyclic plastic zone radius is proportional to ΔK_I^2, where ΔK_I is the range of variation of the Mode I stress intensity factor. Consequently, the dissipated power per unit length of crack front is proportional to the stress intensity factor variation to the power four:

$$q = q_0 \Delta K^4, \tag{2}$$

with

$$q_0 = \frac{\eta f}{8^2 \pi^2 \sigma_y^4} \tag{3}$$

for plane stress conditions and,

$$q_0 = \frac{\eta f}{24^2 \pi^2 \sigma_y^4} \tag{4}$$

for plane strain conditions.

These results have been already shown analytically [7] and numerically [8]. Furthermore it is important to note that Pippan and Stüwe [9] have also proved these results by experiments. In particular, with crack growth experiments at two loading frequencies (50 and 250 Hz) under two R ratios (0.1 and 0.5), on CT specimens made of two steels (named St 70 and St 37), Pippan and Stüwe have shown that: (i) under cyclic loading, most of the plastic work is dissipated in heat, (ii) the plastic work per cycle and per unit of specimen thickness is proportional to ΔK^4, and (iii) this plastic work is R ratio independent.

A constant heat source is considered in the present paper and, in such a case, an analytical solution for our problem exists. Furthermore, note that, in general, the fatigue crack velocity is small, especially when the stress intensity range ΔK is close to the threshold value ΔK_{th}. Since q is proportional to ΔK^4, for a slow moving crack, ΔK and also the heat source q can be supposed constant. Moreover, in such case the heat source associated with the fatigue crack propagation can also be supposed to be motionless. This assumption can be justified by the calculation of the Péclet number, noted Pe, which compares the characteristic time of thermal diffusion with the characteristic time associated to the heat source velocity (i.e. the velocity of the reverse cyclic plastic zone at the crack tip). In this case, the Péclet number is expressed by:

$$Pe = \frac{Lv}{a}, \tag{5}$$

where L is the characteristic length of crack propagation, v the crack velocity and a the thermal diffusivity. For a crack length of $1\,mm$, a crack velocity of $0.1\,mms^{-1}$ and a thermal diffusivity of $1.5 \times 10^{-5}\,m^2s^{-1}$ (typical value for steel), it is possible to calculate a Péclet number equal to 6×10^{-3}. This value remains small compared to unity and, therefore, the heat source can also be considered as motionless.

Within all these assumptions, the thermal problem is axisymmetric. The authors [6] have solved the associated heat transfer equation considering that there is a homogeneous temperature T_0 in the plate at time $t = 0$. The temperature variation field $\vartheta(r,t) = T(r,t) - T_0$ can be expressed by:

$$\vartheta(r,t) = \frac{-q}{4\pi\lambda} \mathrm{Ei}\left(-\frac{r^2}{4at}\right), \tag{6}$$

with $a = \frac{\lambda}{\rho C}$ is the heat diffusivity (ρ is the density of the material, C its heat capacity, λ its heat conductivity) and $-\mathrm{Ei}(-x) = \int_x^\infty \frac{\mathrm{e}^{-u}}{u}\mathrm{d}u$ the integral exponential function. It has to be noticed that the temperature is proportional to the dissipated power q.

2.2. The stress field due to the heterogeneous temperature field near the crack tip

2.2.1. Hypothesis

The temperature field associated with the heat source in the reverse cyclic plastic zone generates a temperature gradient varying with time outside this plastic zone and, consequently, creates thermal stresses due to the thermal expansion of the material. In order to estimate these thermal stresses, the thermo-mechanical problem with the temperature field previously calculated has been solved by Ranc et al. [6]. This thermo-mechanical problem is supposed to be bi-dimensional because the temperature field is axisymmetric. Indeed, the theoretical problem of an infinite plate with a semi-infinite through crack under Mode I cyclic loading is considered (Figure 1). The material is assumed to be homogeneous and isotropic with an elastic-plastic behavior, and plastic strain occurs only in the reverse cyclic plastic zone (cylinder domain with radius r_R).

In both cases of plane stress and plane strain, there is unrestricted plastic flow through the thickness direction in the cracked specimen. With alternating plasticity, the mean radial stress in the reverse cyclic plastic zone tends toward to zero (i.e. mean stress relaxation). Also in the thermo-mechanical problem, only the elastic domain is considered and the boundary condition in the reverse cyclic plastic zone radius is the following: the radial stress is equal to zero.

Further, since the constitutive behavior of the material is supposed to be isotropic and thermo-elastic, it is expected in first approximation that, outside of the reverse cyclic plastic zone, the basic equations of thermo-elasticity govern the problem. Two particular stress strain cases are considered for the elastic region: (i) plane stress where the normal stress (σ_z) is equal to zero, and (ii) plane strain where the strain (ε_z) is equal to zero. In both cases, the material behavior outside the reverse cyclic plastic zone is modeled by an isotropic thermo-elastic stress strain law. The plane stress case is adopted here for the sake of simplicity. For more details the readers may read Ref. [6] for the plane strain case that was examined by Ranc et al. in 2010.

2.2.2. The analytical solution of the thermo-mechanical problem

Ranc et al. [6] have solved the thermo-mechanical problem. The radial and circumferential normal stresses are:

$$\sigma_r(r,t) = \frac{\alpha' E' a q}{\pi \lambda r^2}\left[\frac{t}{2}\left(e^{\frac{-r^2}{4at}} - e^{\frac{-r_R^2}{4at}}\right) + \frac{1}{8a}\left(r^2\mathrm{Ei}(\frac{-r^2}{4at}) - r_R^2\mathrm{Ei}(\frac{-r_R^2}{4at})\right)\right], \tag{7}$$

$$\sigma_\theta(r,t) = \frac{-\alpha' E' q}{8\pi\lambda r^2}\left\{4at\left(e^{-\frac{r^2}{4at}} - e^{-\frac{r_R^2}{4at}}\right) + \left[-r_R^2 \mathrm{Ei}\left(\frac{-r_R^2}{4at}\right) - r^2 \mathrm{Ei}\left(\frac{-r^2}{4at}\right)\right]\right\}, \quad (8)$$

where $E' = E$ and $\alpha' = \alpha$ for plane stress, for Young Modulus E, and linear coefficient of thermal expansion α, whereas $E' = \frac{E}{1-\nu^2}$ and $\alpha' = \alpha(1+\nu)$ for plane strain. In Ref. [6] the circumferential normal stress is then calculated for Young modulus E and Poisson ratio ν equal to the following typical values for steel: $210\,GPa$ and 0.29. The thermal expansion of the material is chosen equal to the typical value $\alpha = 1.2 \times 10^{-5}\,K^{-1}$, and the line heat source is taken equal to the unity ($q = 1\,W.m^{-1}$). Figure 2a shows the evolution of the circumferential stress (i.e. opening stress for the crack) along a radial axis for two different times. Near the reverse cyclic plastic zone ($r_R = 4\,\mu m$) the material is under compression due to the thermal expansion and the constraint effect. Further from this zone, the temperature is lower and the circumferential stress becomes positive (tension) due to the confinement of the material near the crack tip (figure 2a). It has to be pointed out that all the previous illustrated stress values are small because they are computed for a unit heat source q (per unit length of crack front), and the stresses are proportional to q (see Equations 7 and 8) .

2.3. The effect of the thermal stresses on the stress intensity factor under cyclic loading

Within the heterogeneous stress field due to the thermal stresses, for the theoretical case of an infinite plate with a semi-infinite through crack along a radial line from r_R to $+\infty$, it is possible to determine the associated stress intensity factor, $K_{I,temp}$, due to the temperature gradient from the wedge force (Green's function) solution ([10] page 87) as follows:

$$K_{I,temp}(t) = \sqrt{\frac{2}{\pi}}\int_{r_R}^{\infty} \frac{\sigma_\theta(r,t)}{\sqrt{r-r_R}}\mathrm{d}r. \quad (9)$$

From Equations (8) and (9), the stress intensity factor due to thermal stresses is expressed by:

$$\begin{aligned} K_{I,temp}(t) = & \frac{-\alpha' E' q}{8\pi\lambda}\sqrt{\frac{2}{\pi}}\left[\int_{r_R}^{\infty} \frac{4at}{r^2\sqrt{r-r_R}}\left(e^{-\frac{r^2}{4at}} - e^{-\frac{r_R^2}{4at}}\right)\mathrm{d}r\right. \\ & \left. + \int_{r_R}^{\infty} \frac{1}{r^2\sqrt{r-r_R}}\left(-r_R^2 \mathrm{Ei}\left(\frac{-r_R^2}{4at}\right) - r^2 \mathrm{Ei}\left(\frac{-r^2}{4at}\right)\right)\mathrm{d}r\right]. \end{aligned} \quad (10)$$

After integration Ranc et al. [6] have shown that it becomes:

$$K_{I,temp}(t) = \frac{\alpha' E' q}{80\lambda}\sqrt{\frac{2}{\pi}}\left\{40\sqrt{r_R} + \frac{20at(e^{\frac{-r_R^2}{4at}}-1)}{r_R^{3/2}} + 5\sqrt{r_R}\mathrm{Ei}\left(\frac{-r_R^2}{4at}\right)\right.$$
$$+\frac{10(at)^{1/4}}{\Gamma\left(\frac{7}{4}\right)}\left(-3\,{}_2F_2\left[\left(\frac{-1}{4},\frac{1}{4}\right),\left(\frac{1}{2},\frac{3}{4}\right),\left(\frac{-r_R^2}{4at}\right)\right]\right)$$
$$+\frac{10(at)^{1/4}}{\Gamma\left(\frac{7}{4}\right)}\left({}_2F_2\left[\left(\frac{1}{4},\frac{3}{4}\right),\left(\frac{1}{2},\frac{7}{4}\right),\left(\frac{-r_R^2}{4at}\right)\right]\right)$$
$$-\frac{8r_R}{(at)^{1/4}\Gamma\left(\frac{1}{4}\right)}\left(5\,{}_2F_2\left[\left(\frac{1}{4},\frac{3}{4}\right),\left(\frac{5}{4},\frac{3}{2}\right),\left(\frac{-r_R^2}{4at}\right)\right]\right)$$
$$\left.-\frac{8r_R}{(at)^{1/4}\Gamma\left(\frac{1}{4}\right)}\left({}_2F_2\left[\left(\frac{3}{4},\frac{5}{4}\right),\left(\frac{3}{2},\frac{9}{4}\right),\left(\frac{-r_R^2}{4at}\right)\right]\right)\right\}, \tag{11}$$

with the hyper-geometric function

$${}_pF_q\left(\{a_1,...,a_p\};\{b_1,...,b_q\};z\right) = \sum_{k=0}^{+\infty}\frac{(a_1)_k...(a_p)_k}{(b_1)_k...(b_q)_k}\frac{z^k}{k!}, \tag{12}$$

where $(a)_k = \frac{\Gamma(a+k)}{\Gamma(a)} = a(a+1)(a+2)...(a+k-1)$ is the Pochhammer symbol, and $\Gamma(x) = \int_0^{+\infty} u^{x-1}e^{-x}du$ is the Euler Gamma function. For instance, in our case: ${}_2F_2\left(\{a_1,a_2\};\{b_1,b_2\};z\right) = \sum_{k=0}^{+\infty}\frac{(a_1)_k(a_2)_k}{(b_1)_k(b_2)_k}\frac{z^k}{k!}$.

The evolution of $K_{I,temp}$ (the thermal correction on K_I) against time is illustrated in Figure 3 from [6] for a unit line heat source ($q = 1\,Wm^{-1}$) and the following typical material characteristics: $\rho = 7800\,kg.m^{-3}$, $C = 460\,JK^{-1}kg^{-1}$, $\lambda = 52\,Wm^{-1}K^{-1}$, $\alpha = 12\times10^{-6}$ and $E = 210\,GPa$. Figure 3 shows that $K_{I,temp}$ is not very sensitive to the size of the reverse cyclic plastic zone. This is due to the large sizes of the plate considered in this paper.

The $K_{I,temp}$ determined by this equation would be a value superimposed on the usual stress intensity factor due to the cyclic loading, noted $K_{I,cyc}$ in Mode I.

$$K_I(t) = K_{I,temp}(t) + K_{I,cyc}(t) \tag{13}$$

As is written before, due to the compressive thermal stresses around the crack tip, it has been shown that the stress intensity factor during fatigue loading has to be corrected by the factor $K_{I,temp}$.

$K_{I,temp}$ varies with time and can be considered as constant for long times. In the very beginning of loading, the value of $K_{I,temp}$ is small compared with $K_{I,cyc}$ and $\Delta K_I(t) \approx \Delta K_{I,cyc}$. There is also no significant effect of the temperature on the range of the stress intensity factor. For long time ($t >> 0$), $K_{I,temp}$ can be considered as constant during a loading period.

Consequently the temperature has no effect on ΔK_I but it has an effect on $K_{I,max}$ and $K_{I,min}$:

$$K_{I,max} = K_{I,cyc\,max} + K_{I,temp}, \tag{14}$$

$$K_{I,min} = K_{I,cyc\,min} + K_{I,temp}, \tag{15}$$

where $K_{I,min}$ and $K_{I,max}$ are the minimum and the maximum value of $K_I(t)$ over a loading period. However, $K_{I,temp}$ can affect crack closure by changing the load ratio $R_K = \frac{K_{I,min}}{K_{I,max}}$. The ratio R_K is affected by the temperature correction:

$$R_K = \frac{K_{I,min}}{K_{I,max}} = \frac{K_{I,cyc\,min} + K_{I,temp}}{K_{I,cyc\,max} + K_{I,temp}} \neq \frac{K_{I,cyc\,min}}{K_{I,cyc\,max}} \tag{16}$$

The evaluation of this correction needs a precise quantification of the heat source associated with the plastic dissipation and the thermal boundary conditions at the border of the plate. Experimental measurements of the temperature field, for instance by using pyrometry technique, need to be carried out in this way, and a more representative case study should be considered because a real structure is not infinite and is submitted to thermal losses (convection for instance). Such a study is proposed in the following section.

3. A finite plate with a central through crack

For being representative of a real propagating crack problem, let us now consider a finite plate with a central through crack. The fatigue crack growth tests carried out in this study are first presented in the following together with the measurement of the temperature field at the surface of the cracked specimen. In such a case, thermal losses due to convection cannot be neglected. That is the reason why the computation of both the temperature field and the associated stresses and strains have been done by a finite element analysis as presented in the previous section and Ref. [6]. The results of these calculations and the identification of the heat source are presented in the third and fourth part of this section. Finally, the correction on the Mode I stress intensity factor is estimated.

3.1. Heat source identification associated with the fatigue crack growth

3.1.1. Experimental conditions

Fatigue crack growth tests have been carried out on a plate specimen made of a mild steel (C40) in order to estimate the dissipated power per unit length of the crack front during cyclic loading. The mechanical properties of this steel are the following: Young modulus $E = 210$ GPa, Yield stress $\sigma_y = 350$MPa, ultimate tensile strength UTS=600 MPa. A center cracked specimen is used with a thickness of $4\,mm$ as is illustrated Figure 4. The fatigue tests have been carried out at room temperature (around $20°C$) with a resonant fatigue testing machine

(Vibrophore). The loading frequency is about 100 Hz. The temperature field at the specimen surface is measured with an infrared camera (CEDIP Jade III MWR) whose spectral range is between $3.9\,\mu m$ and $4.5\,\mu m$. The acquisition frequency and the aperture time of the camera are respectively $5Hz$ and $1100\,\mu s$. In order to neglect the effect of the emissivity of the surface on the determination of the temperature, the specimen is covered with a fine coat of mat black paint. The specimen is pre-cracked under cyclic loading at R=0 so that an additional natural fatigue crack of 2 mm occurs at each end of the initial central crack machined by electro-erosion (Figure 4).

The experimental conditions of the tests are summarized in Table 1. The length of the initial crack a_{ini} and the final length a_{end} are measured with a high resolution optical camera. ΔK_{int} and ΔK_{end} are calculated from respectively a_{ini} and a_{end}. All the infrared measurements are carried out on the left-hand side crack, but the two cracks emanating from the center of the plate are measured. Their length is quite the same, the maximum difference is lower than 0.5 mm (therefore this is not reported in Table 1).

Test reference	R Ratio	Test duration $[s]$	a_{ini} $[mm]$	ΔK_{ini} $[MPa\sqrt{m}]$	a_{end} $[mm]$	ΔK_{end} $[MPa\sqrt{m}]$	N [cycles]
E1	0.1	1600.0	16.5	12	17.1	12.5	160×10^3
E2	0.1	766.0	17.1	15	19.1	15.8	76.6×10^3
E3	0.1	828.8	19.1	17	21.9	18.2	82.88×10^3
E4	0.1	689.4	21.9	20	26.3	21.8	68.94×10^3

Table 1: Experimental conditions.

3.1.2. Temperature field around the crack tip

Figure 5a presents the mean temperature evolution at the crack tip in the case of the test E4 in each of the five areas near the crack front defined in Figure 5b. The temperature evolution exhibits a superposition of a high frequency evolution of the temperature due to the thermoelasticity and a low frequency signal evolution corresponding to the dissipated power in the reverse cyclic plastic zone. Indeed, under cyclic stress, the thermoelastic effect generates a reversible variation of the temperature. Since the acquisition frequency is much weaker ($5\,Hz$) than the smallest requested frequency (approximately $200\,Hz$), the temperature oscillation frequency is controlled by the stroboscopic effect. Consequently this frequency depends on the loading frequency of the machine and the acquisition frequency of the camera. The amplitude of the temperature oscillations depends directly on the stress amplitude and more precisely on the stress tensor trace. Figure 5a illustrates clearly that, when the distance from the crack tip increases, the amplitude of the temperature oscillations decreases because the amplitude of the

local stresses decreases also. However, these oscillations remain low compared with the average temperature increase that is the consequence of the dissipation in heat and that is of interest in this paper.

The total increase of the temperature in the specimen between the beginning and the end of the test corresponds to the heat source related to the plastic dissipation in the reverse cyclic plastic zone. This heat diffuses in all the specimen and generates an increase of its temperature. Figure 6 shows the temperature field variation between the beginning and the end of the test E4 on the surface specimen near the crack front. It can be noted that the temperature is not homogeneous close to the crack tip.

For a range of the Mode I stress intensity factor, ΔK of $20\,MPa\sqrt{m}$ and R ratio equal to 0.1, the total increase in the temperature is about $2.5°C$ in the area number 2 (defined by Figure 5b). At the end of the test, the cyclic loading is stopped and the specimen cools freely under the effect of convection.

Furthermore, it has to be noticed that constant amplitude fatigue tests have been carried out on a mat black paint smooth specimen (made of the same C40 steel, with the same thickness) without any crack. The same fatigue testing machine has been used at the same loading frequency. For the same nominal stress amplitudes as those applied on the cracked specimen, no self heating is measured by the infrared camera. Indeed, it is known in the literature that, for some metals, self heating could appear at stress level equal to or higher than the fatigue limit [11, 12]. This is not the case in our experiments. The observed temperature increase is due to the heat source at the crack tip.

3.1.3. Identification of the dissipated power from the temperature measurement

In order to estimate the dissipated power in the reverse cyclic plastic zone, a thermal modeling of the specimen has been done by FEA (with a home-made finite element model using Matlab). The geometry of the modeled specimen and the thermal boundary conditions are shown in Figure 7. The sizes of the simulated specimen are similar to those of the tested specimen (Figure 4). The temperature is supposed to be homogeneous in the thickness of the specimen, and a two dimensional calculation is then carried out. Due to the symmetry of the problem, only one fourth of the specimen is modeled. Convection boundary conditions are considered all around the specimen (edge of the specimen and on the surface of the specimen). The convective heat transfer coefficient, noted h, is taken equal to $10\,Wm^{-2}K^{-1}$ (typical value for natural convection in air). For mild steel, the density, the heat capacity and the thermal conductivity are taken equal to respectively $7800\,kg.m^{-3}$, $460\,J.K^{-1}.kg^{-1}$ and $52\,W.m^{-1}.K^{-1}$.

Both the initial temperature and the ambient temperature are taken equal to $20°C$. The dissipated power in the reverse cyclic plastic zone is modeled by a line heat source along the crack front (as was done by the authors in [6]). As the thermal problem is linear, a line heat source of $1\,W.m^{-1}$ is applied in the FEA. The thermal problem is consider as stationary and also independent of time.

Figures 8 and 9 show the temperature field on the specimen surface and the temperature evolution along the x axis for a crack position $a = 21.9\,mm$. This geometrical configuration corresponds to the beginning of test E4 with stress ratio $R = 0.1$ and stress intensity factor range $\Delta K = 20\,MPa\sqrt{m}$. The FEA shows that, at a distance of $5\,mm$ of the crack tip (zone 2 on Figure 5), the temperature increase is equal to $0.0163°C$ for a unit dissipated power ($q = 1\,W.m^{-1}$). Since for the test E4, the temperature variation in the same zone is about $2.5°C$, this value allows the following estimation of the dissipated power: $153\,Wm^{-1}$. With the same methodology the temperature variation in zone 2 is measured, and the dissipated power is computed. The results are shown in Table 2 for the four test conditions. Furthermore, Figure 9 shows that the temperature field around the crack tip is strongly heterogeneous.

Test reference	a_{ini} $[mm]$	ΔK_{ini} $[MPa\sqrt{m}]$	Temperature variation in area 2 $[°C]$	Dissipated power $[W.m^{-1}]$
E1	16.5	12	0.3	17.7
E2	17.1	15	1	62.2
E3	19.1	17	1.4	84.1
E4	21.9	20	2.5	153

Table 2: Temperature variation in zone 2 and dissipated power for the different tests.

3.2. Quantification of the stress field associated with the temperature field

3.2.1. Presentation of the method

The cracked specimen is subjected to a cyclic loading, and far from the crack, the normal stress in the direction of the specimen is $\sigma(t) = \sigma_m + \sigma_a \sin(\omega t)$ where σ_m is the mean value of stress, σ_a the stress amplitude and ω the angular frequency. It also appears a heat source along the crack front associated with the plastic dissipation in the reverse cyclic plastic zone. This dissipated power is not constant during one loading cycle but this is always positive because of the second law of thermodynamics. However, if the test duration is supposed to be very much longer than the loading cycle period, it can be considered that the dissipation evolution during one cycle remains small compared to its variation during the test. Moreover, in our calculation the crack is loaded with a quasi-constant stress intensity factor range and a constant stress ratio, that is why the heat source (noted q) is supposed constant during one test.

The dissipated power in the reverse cyclic plastic zone also generates a heterogeneous temperature field which depends on the intensity of the heat source associated with the plasticity and the thermal boundary conditions of the cracked specimen. This temperature field is calculated in the previous section. Due to the thermal expansion of the material, the temperature gradient near the crack tip creates thermal stresses which contribute to the stress field associated with the cyclic loading of the crack.

Plane stress conditions are assumed. In the reverse cyclic plastic zone, there is unrestricted plastic flow through the thickness direction in the cracked specimen. With alternating plasticity in the reverse cyclic plastic zone, the mean stress tends toward to zero. Also in the thermo-mechanical problem, only the elastic domain is considered and the boundary condition in the reverse cyclic plastic zone radius is that the radial stress is equal to zero. The boundary conditions are illustrated in Figure 7. Outside the reverse cyclic plastic zone, the constitutive behaviour of the material is thermo-elastic. The Young modulus, Poisson ratio, density and thermal expansion coefficient are respectively equal to $210\,GPa$, 0.29, $7800\,kg.m^{-3}$, and $1.2 \times 10^{-5}\,K^{-1}$.

This thermo-mechanical problem can be decomposed into two problems : the first problem (purely mechanical problem) is the cracked specimen subjected only to the cyclic loading $\sigma(t) = \sigma_m + \sigma_a \sin(\omega t)$ without heat source due to the crack. The stress field associated with this problem is related to a Mode I stress intensity factor $K(t)$. The second problem (purely thermal problem) is the cracked specimen subjected to the line heat source q. The thermal stress associated with this thermal loading is related to a stress intensity factor named K_{temp}. This decomposition is illustrated in Figure 10. This decomposition is correct if there is a small effect of the heat source on the reverse cyclic plastic zone size. The thermal effect generates a compressive stress field near the crack front and thus creates a negative contribution on the stress intensity factor ($K_{temp} < 0$).

The first problem (pure mechanical problem) is solved in a classical way and enables us to estimate the Mode I stress intensity factor $K(t)$ according to the applied stress $\sigma(t)$. The resolution of the second problem and the estimation of K_{temp} are more difficult. The authors have used a solution consisting in another decomposition of the thermal problem into two other problems (Figure 11). In the first case (a), a stress $\sigma(x)$ is applied on the crack lips in order to impose a crack opening equal to zero ($u_y = 0$). This stress $\sigma(x)$ is calculated from a thermoelastic problem without crack and with the heat source q. The stress intensity factor

for case (b) is then calculated with the Green function [10]:

$$K_I(b) = K_{temp} = \frac{2}{\sqrt{\pi}} \int_0^a \sigma(x) \frac{\sqrt{a}}{\sqrt{a^2 - x^2}} \mathrm{d}x \tag{17}$$

3.2.2. Calculation results for the test E4

The results of the calculation of the effect of self heating on the stress intensity factor is now detailed in the particular case of the test E4 with a stress intensity factor range equal to $20\,MPa\sqrt{m}$ (and $R = 0.1$). The temperature field is thus calculated and the mechanical problem (Case (a)) of the thermal problem is solved. Figures 12a and 12b illustrate the evolution of the normal strain ε_{xx} and ε_{yy} respectively, along the x axis. On these two figures, the red curve corresponds to the evolution of the thermal strain due to the thermal expansion.

Figures 13 and 14 show the evolution of the normal thermal stresses σ_{xx} and σ_{yy} (crack opening stress) along the x axis. These figures show clearly that, due to dissipation in heat, the crack tip is under compression. Near the reverse cyclic plastic zone, the radial normal stress is equal to zero (cyclic mean stress relaxation modeled by the boundary conditions on the reverse cyclic plastic zone interface). There is then a minimum of the normal stress at a distance of $40\,\mu m$ from the reverse cyclic plastic zone. Figure 13b shows an enlargement on this minimum of the stress.

3.3. Assessment of the effect on the stress intensity factor

Calculation previously presented has been carried out for all the tests listed in Table 1. From Equation (17) and the thermal stress field (as is illustrated in Figure 14 in the particular case of test E4), the effect of dissipation in heat on the Mode I stress intensity factor, K_{temp}, can be estimated. All the results are shwon in Table 3. They are negative because of the compressive thermal stresses around the crack tip.

In the case of test E4, the correction on the stress intensity factor is $-0.32\,MPa\sqrt{m}$. This table shows that, for the investigated material and experimental conditions, the effect of plastic dissipation in heat at the crack tip is small compared to the range of the stress intensity factor, especially for low value of ΔK. However, it has to be kept in mind that the dissipated power per unit length of the crack front is both proportional to the loading frequency (around 100Hz in the present study) and strongly dependent on the material mechanical properties since it is proportional to σ_y^{-4} (see equations 3 and 4). Consequently this effect could be much more pronounced for ductile materials (low cyclic yield stress) and high values of stress intensity factor range.

Test reference	ΔK $[MPa\sqrt{m}]$	r_R $[\mu m]$	Dissipated power $[Wm^{-1}]$	K_{temp} $[MPa\sqrt{m}]$
E1	12	58	17.7	-0.04
E2	15	90	62.2	-0.14
E3	17	116	84.1	-0.18
E4	20	190	153	-0.32

Table 3: Radius of the reverse cyclic plastic zone, dissipated power and thermal correction of the stress intensity factor computed for the four fatigue crack growth tests at R=0.1

4. Conclusion and prospects

Under cyclic loading, the temperature variation field around the crack tip of a cracked structure is strongly heterogeneous. This is due to the dissipation in heat within the reverse cyclic plastic zone and the thermal stresses induced by the thermal expansion coefficient of the material. It has been shown that, due to the temperature gradient outside the plastic zone, a local compressive stress field is created. Consequently, the Mode I stress intensity factor has to be corrected by a negative value noted K_{temp}. This reduces the crack driving force. The Mode I stress intensity factor has then been calculated by taking into account this field. Both the effective range of the stress intensity factor (considering closure), the maximum and minimum values of K_I and the stress intensity ratio $R_K = \frac{K_{I,min}}{K_{I,max}}$ are affected by the thermal stresses.

In the case of an infinite plate with a semi-infinite through crack under a remotely applied tensile force (Mode I), an analytical expression of this correction factor on the Mode I stress intensity factor exists. This is proportional to the heat source, q, in the reverse cyclic plastic zone. For a finite plate with a large central through crack a finite element analysis, which takes into account the convection heat losses, both the temperature field and the induced thermal stresses responsible for K_{temp} are needed to be computed. Experimental investigations have been carried out on a mild steel (C40). They show that the heat source under $\Delta K = 20$ MPa$\sqrt{m}$ and R=0.1 is small ($\approx -0.32\, MPa.\sqrt{m}$).

However, since the dissipated power per unit length of the crack front is proportional to both the loading frequency and $(\Delta K/\sigma_y)^4$, this effect should be more important for ductile metals (low yield stress) loaded under high stress intensity factor range. Revisiting the frequency effect on the fatigue crack growth could be also interesting by taking this thermal correction into account. According to the authors, systematic experiments should be carried out on several materials to quantify the heat source at the crack tip which is clearly a key factor in fracture mechanics, especially for fatigue crack growth tests at high frequency. Other studies should be carried out in thermomechanics to take into account the temperature field effect on

fracture mechanics considerations. Furthermore, additional studies have to be done to compute the thermal stresses around the crack tip of a cracked structure under non-stationary regime. The thermomechanical problem with a moving heat source on a finite plate has also to be investigated.

Acknowledgements

The authors acknowledge Arts et Métiers ParisTech and Foundation Arts et Métiers for the financial support of Paul C. Paris' stay at the Bordeaux Center of Arts et Métiers ParisTech.

References

References

[1] W. S. Farren, G. I. Taylor, The heat developed during plastic extension of metals, Proceedings of the Royal Society A 107 (1925) 422–451.

[2] G. I. Taylor, H. Quinney, The latent energy remaining in a metal after cold working, Proceedings of the Royal Society A 143 (1934) 307–326.

[3] P. Paris, Fatigue - The Fracture Mechanics Approach, Fatigue an Interdisciplinary Approach, Syracuse University Press, 1964.

[4] J. Rice, Fatigue Crack Propagation, ASTM, Special Technical Publication 415, Philadelphia, 1967, Ch. The Mechanics of Crack Tip Deformation and Extension by Fatigue, pp. 247–311.

[5] W. Elber, Fatigue crack closure under cyclic tension, Engineering Fracture Mechanics 2 (1) (1970) 37–45.

[6] N. Ranc, T. Palin-Luc, P. Paris, Thermal effect of plastic dissipation at the crack tip on the stress intensity factor under cyclic loading, Engineering Fracture Mechanics 78 (2011) 961–972.

[7] N. Ranc, D. Wagner, P. C. Paris, Study of thermal effects associated with crack propagation during very high cycle fatigue tests, Acta Materialia 56 (15) (2008) 4012–4021.

[8] N. W. Klingbeil, A total dissipated energy theory of fatigue crack growth in ductile solids, International Journal of Fatigue 25 (2) (2003) 117–128.

[9] R. Pippan, Stüwe, Thermische bestimmung der plastischen deformation um die rissfront eines ermüdungsbruches, Zeitchrift für Metallkunde (1983) 699–704.

[10] H. Tada, P. C. Paris, G. R. Irwin, The stress analysis of cracks handbook, A.S.M.E. Press, 2000.

[11] M. Luong, Fatigue limit evaluation of metals using an infrared thermographic technique, Mechanics of Materials 28 (1988) 155–163.

[12] G. La Rosa, A. Risitano, Thermographic methodology for rapid determination of the fatigue limit of materials and mechanical components, International Journal of Fatigue 22 (2000) 65–73.

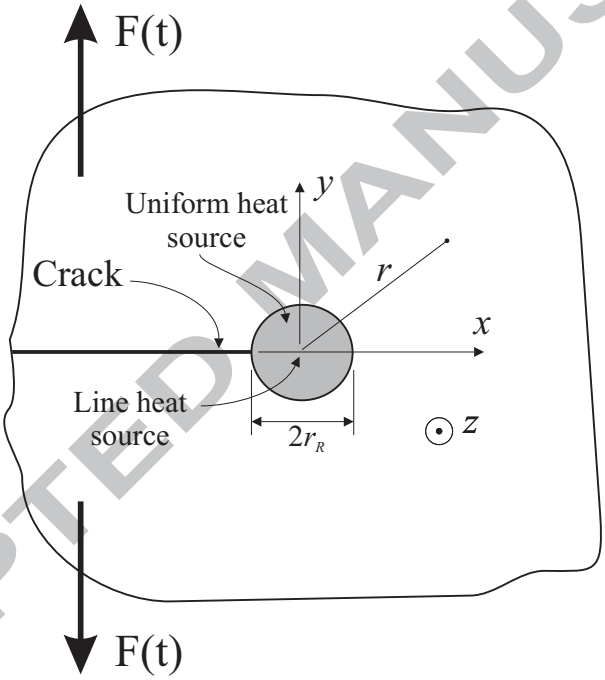

Figure 1: Schematic of the thermodynamical problem of a semi-infinite crack in an infinite plate under cyclic tension (Mode I) caused by a remote mechanical loading $F(t)$.

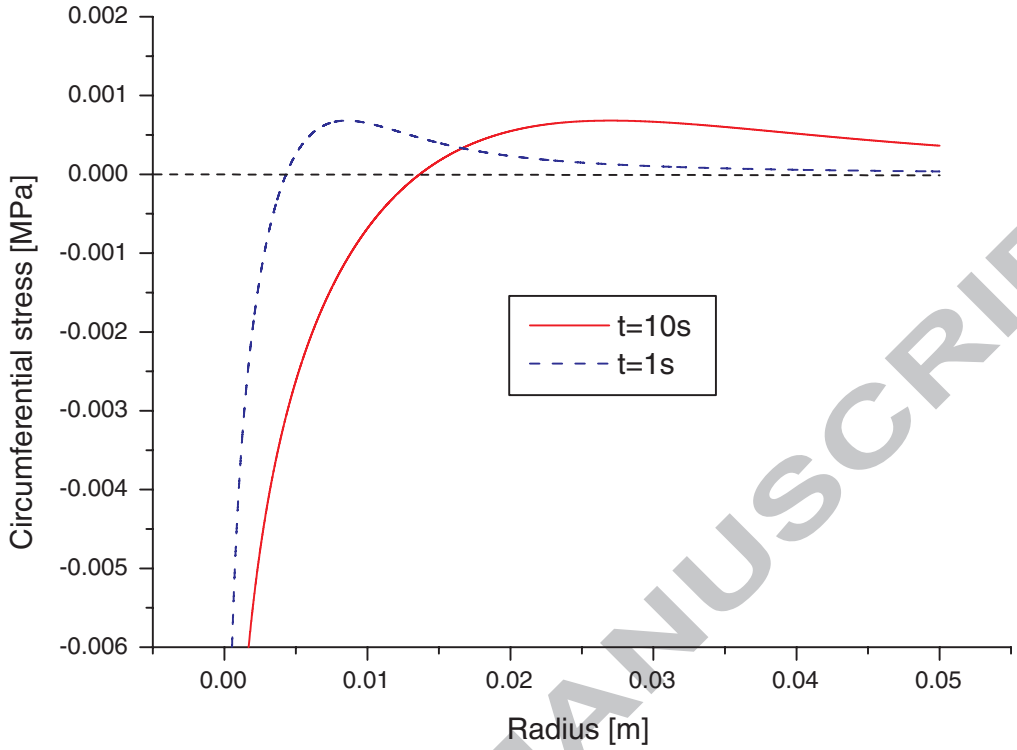

a)

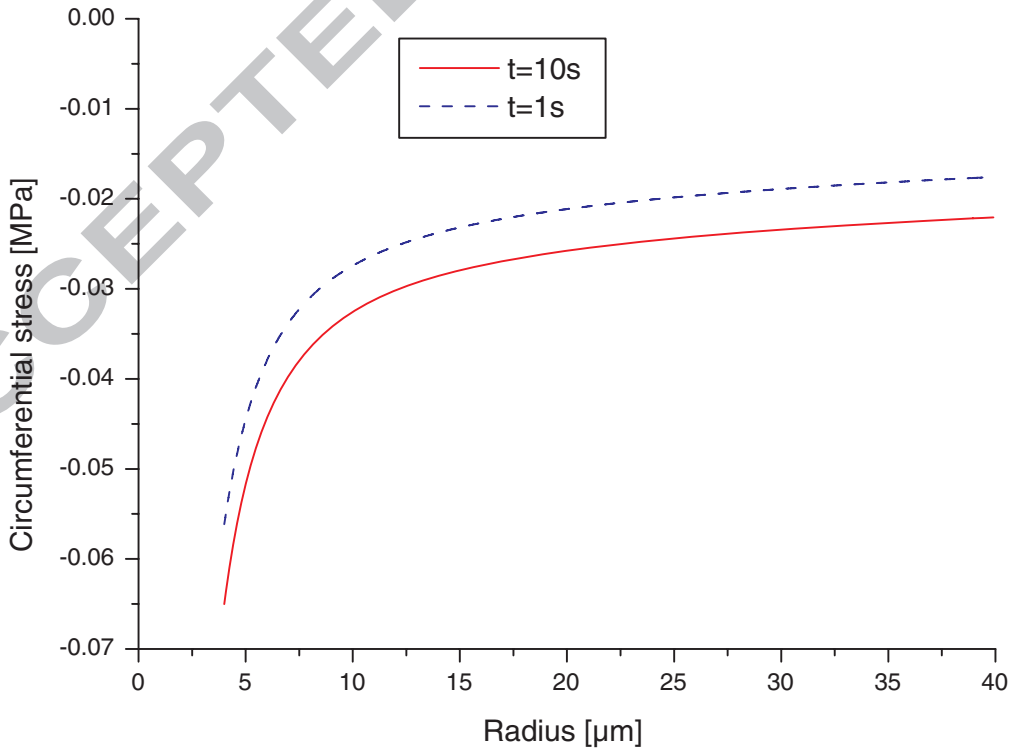

b)

Figure 2: The circumferential stress distribution at various times for a unit heat source $q = 1\,Wm^{-1}$ and $r_R = 4\,\mu m$: (a) general view, (b) enlargement near the reverse cyclic plastic zone, from [6].

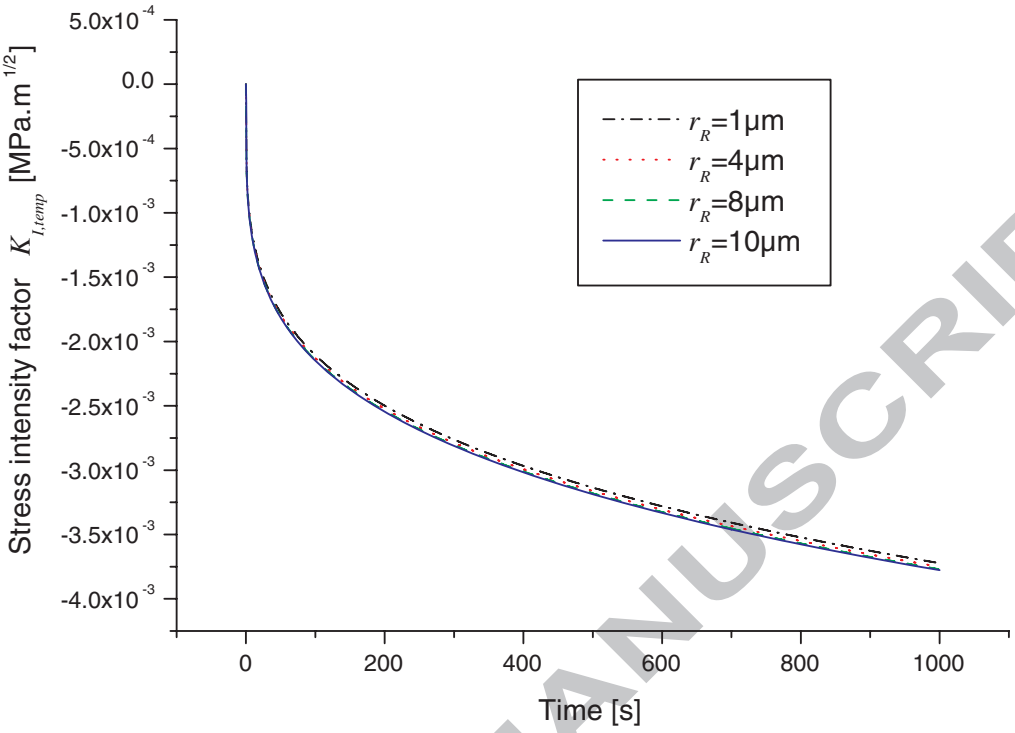

Figure 3: The stress intensity factor $K_{I,temp}$ due to thermal stresses versus time for different radius of the reverse cyclic plastic zone, from [6].

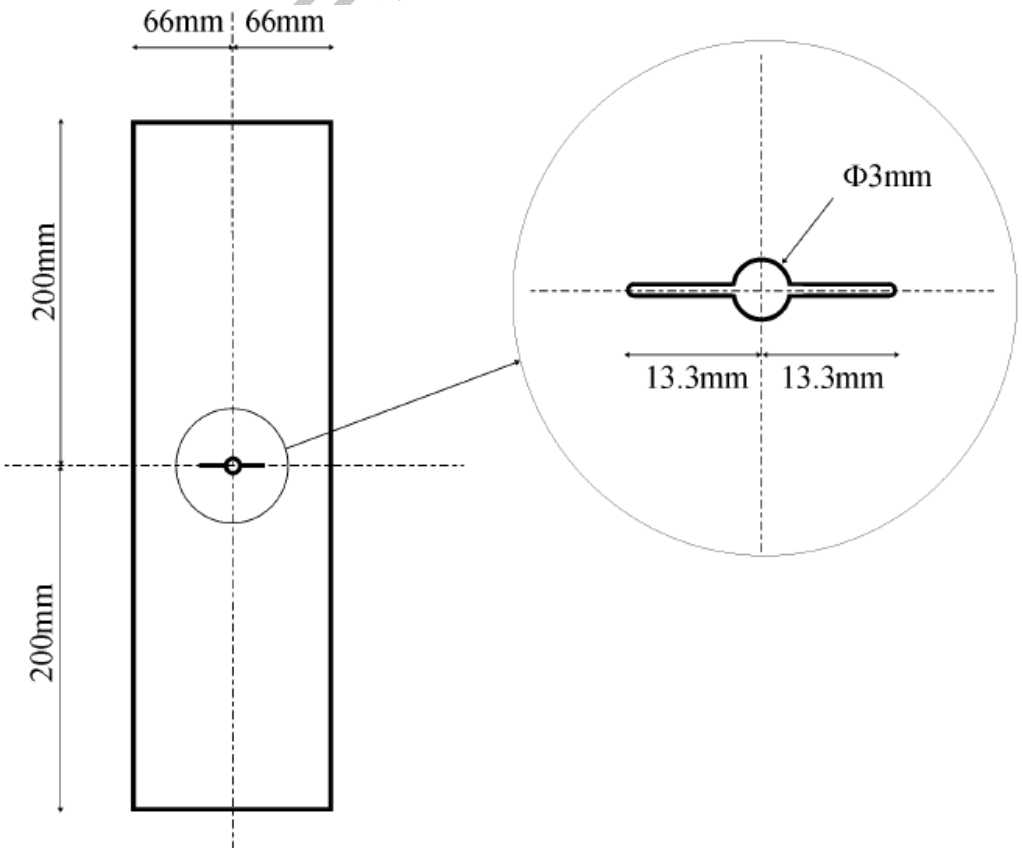

Figure 4: Geometry of the center cracked specimen made of C40 steel (thickness 4 mm).

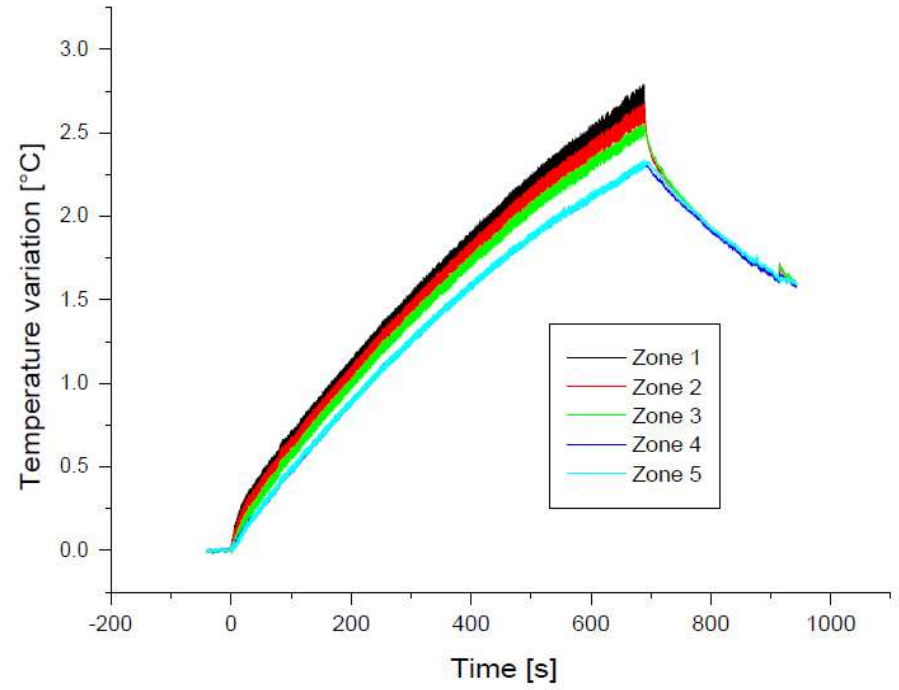

a)

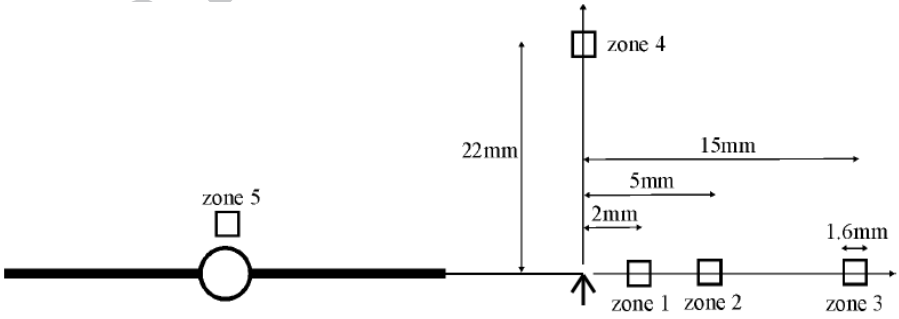

b)

Figure 5: Temperature results: (a) temperature evolution during test E4 ($\Delta K = 20\,MPa\sqrt{m}; R = 0.1$), (b) location of the different areas used in Figure 5a). The arrow indicates the crack tip position.

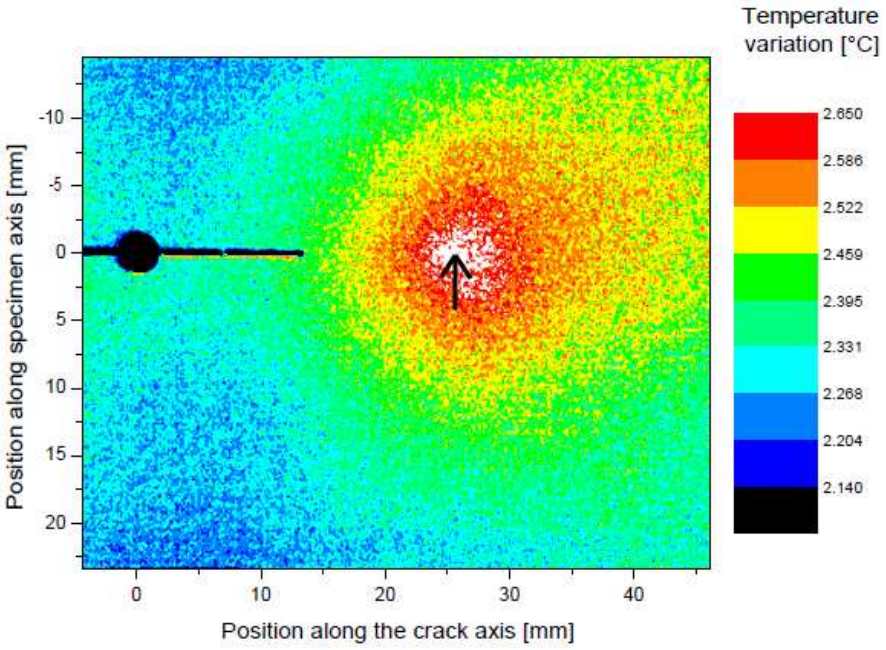

Figure 6: Temperature variation field near the crack front for the test E4 ($\Delta K = 20\,MPa\sqrt{m}; R = 0.1$). The arrow indicates the tip of the natural fatigue crack emanating from the crack machined by electro-erosion (on the left).

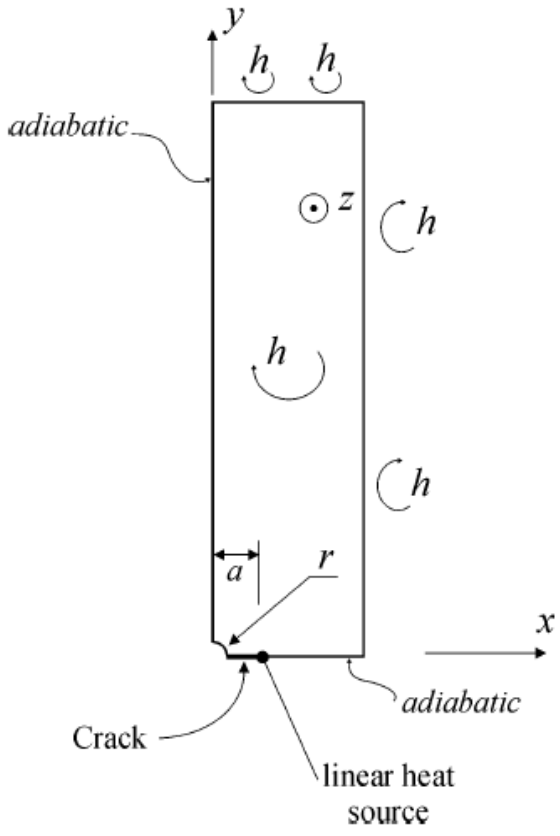

Figure 7: Geometry and boundary conditions of the thermal problem.

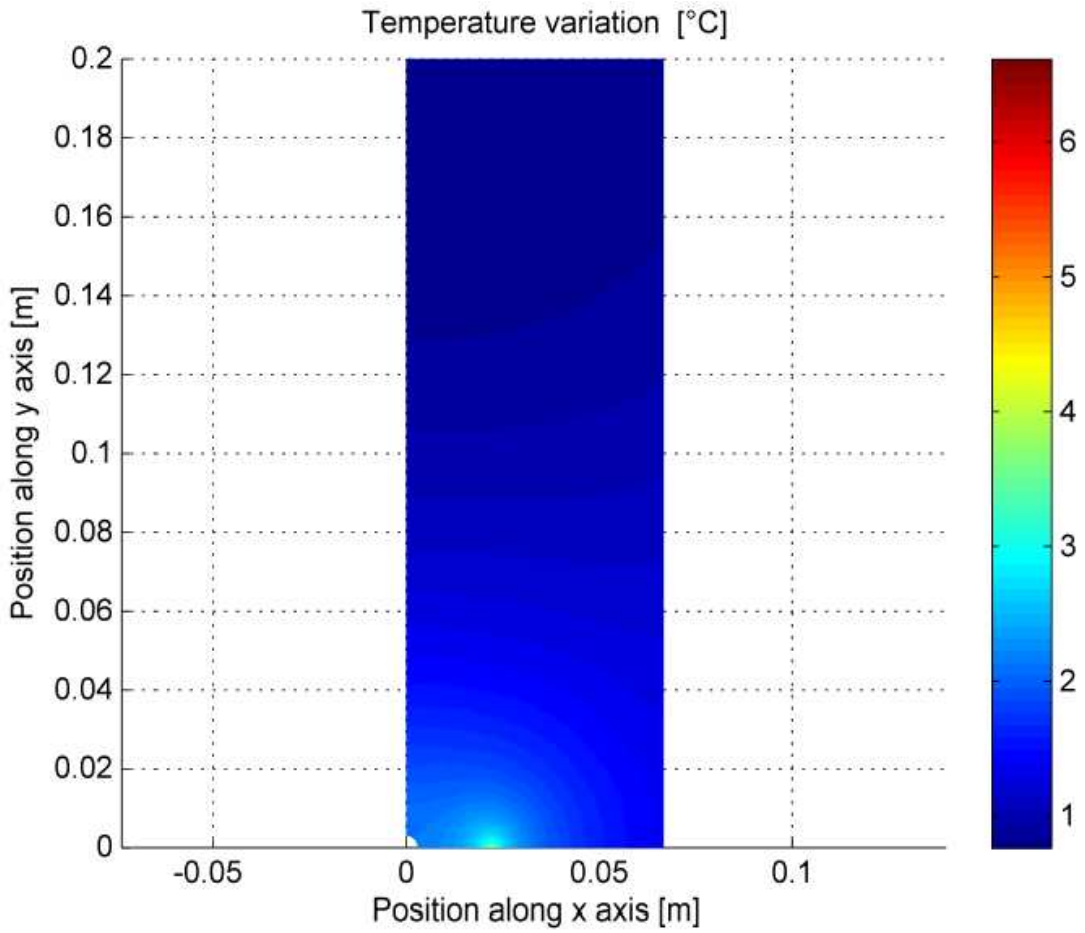

a)

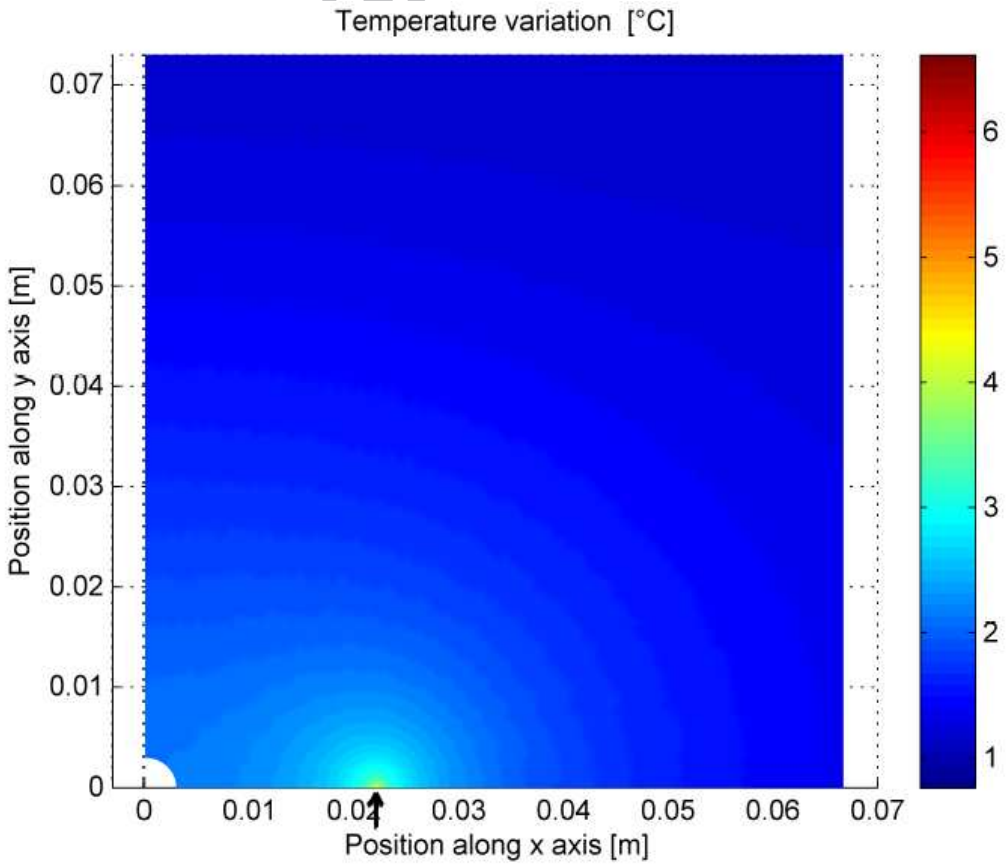

b)

Figure 8: Temperature field computed on the specimen surface for a unit heat source: (a) general view, (b) enlargement (the arrow shows the crack tip position).

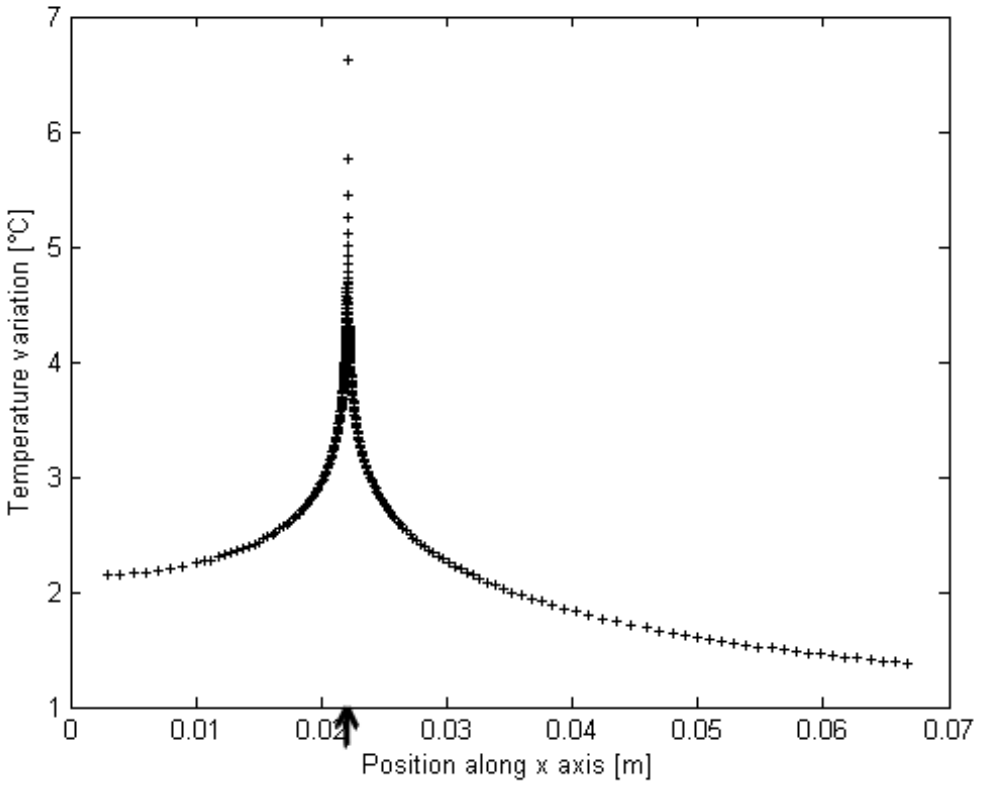

Figure 9: Temperature variation field evolution along the x axis for test E4 (the arrow indicates the crack tip position on the x axis).

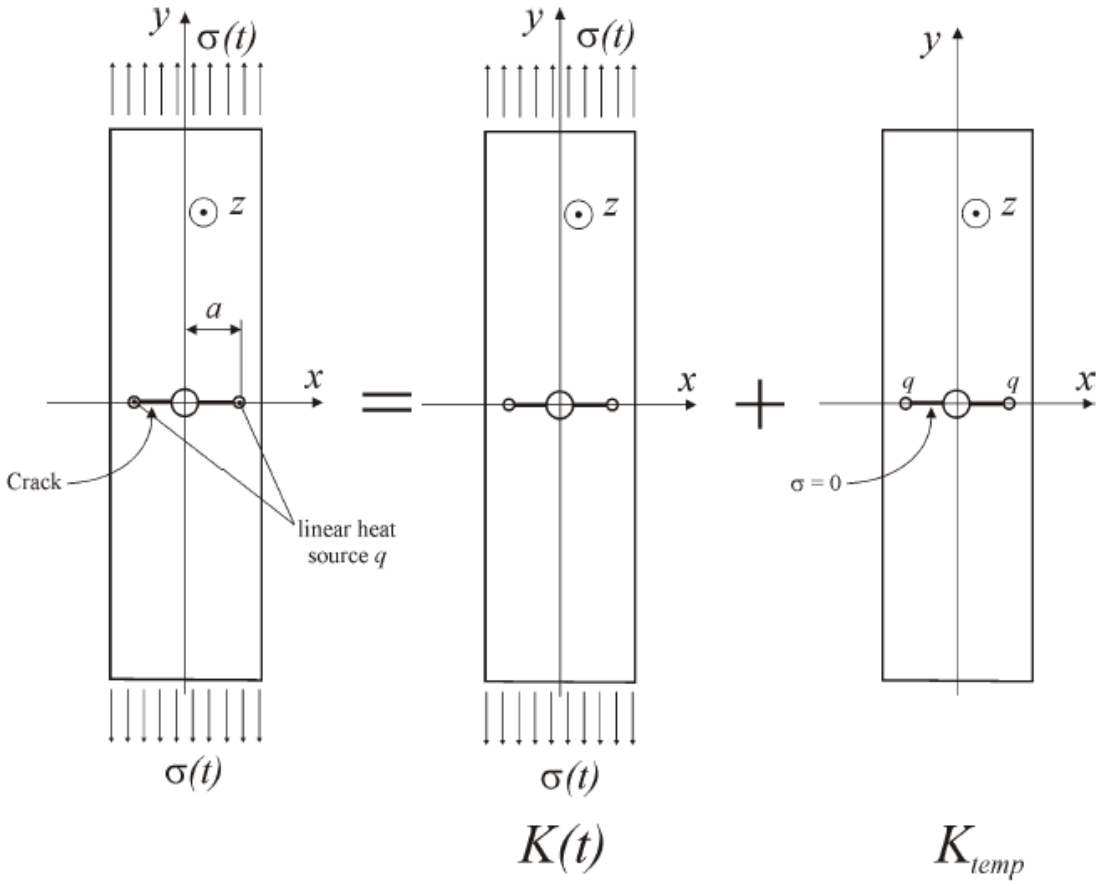

Figure 10: Decomposition of the general problem in a mechanical problem and a thermal problem.

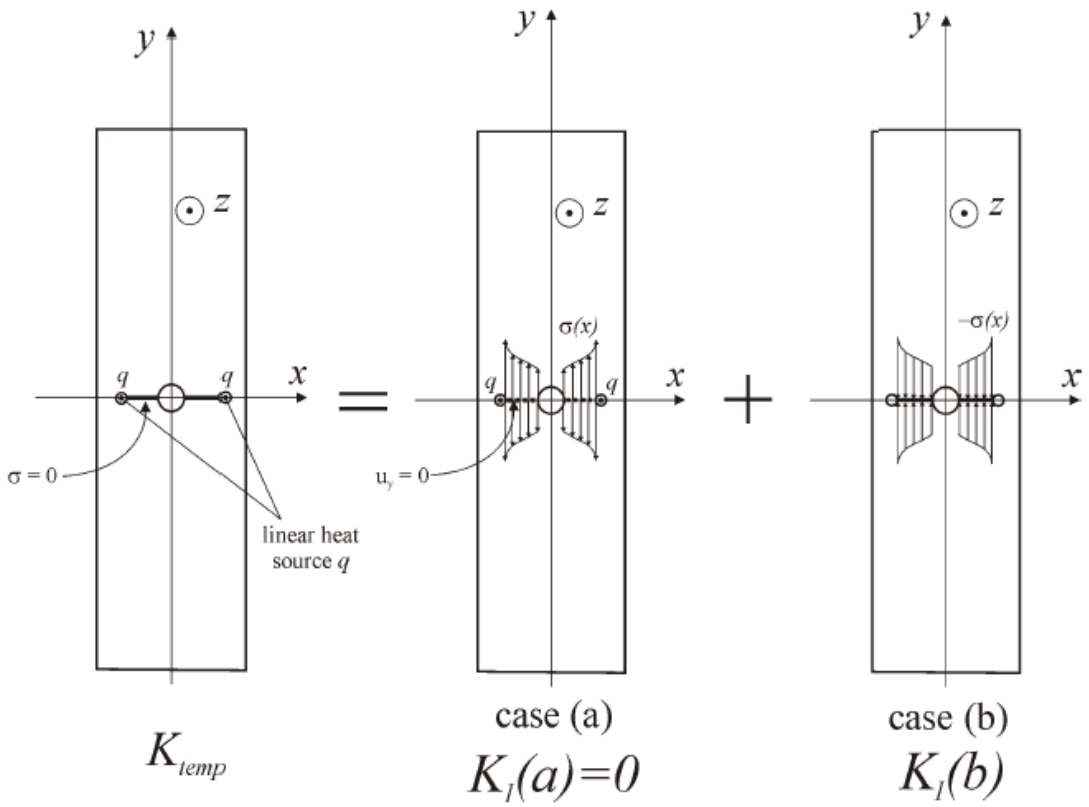

Figure 11: Decomposition of the thermal problem into two other problems.

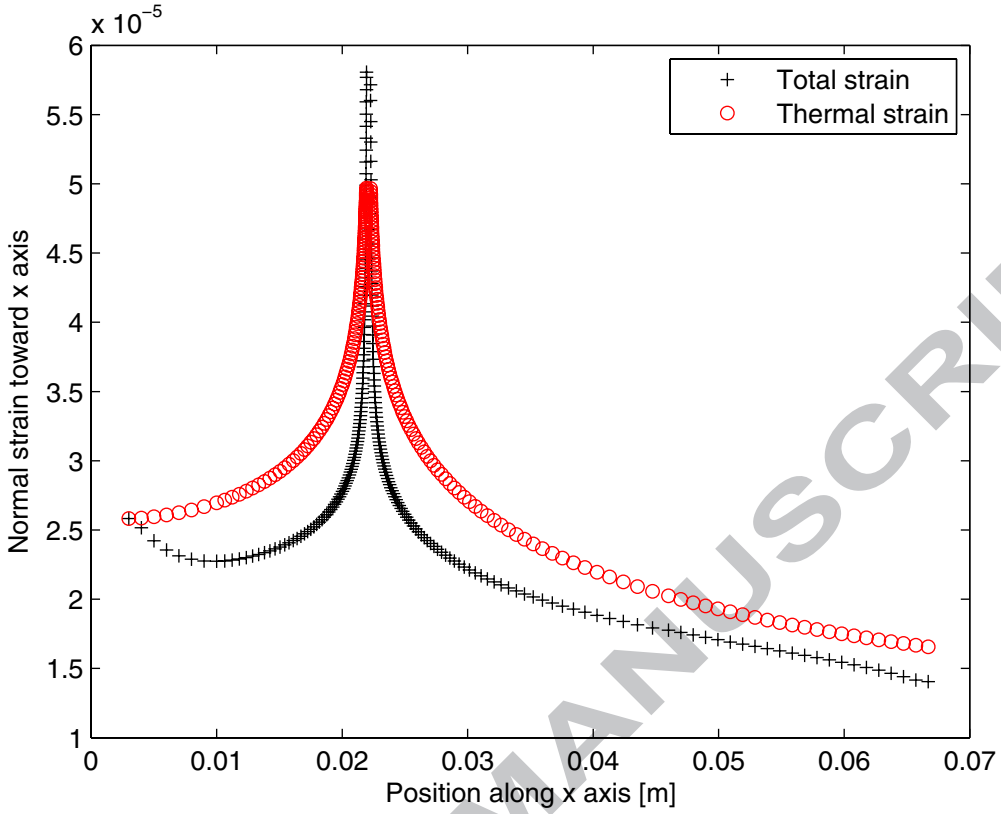

a)

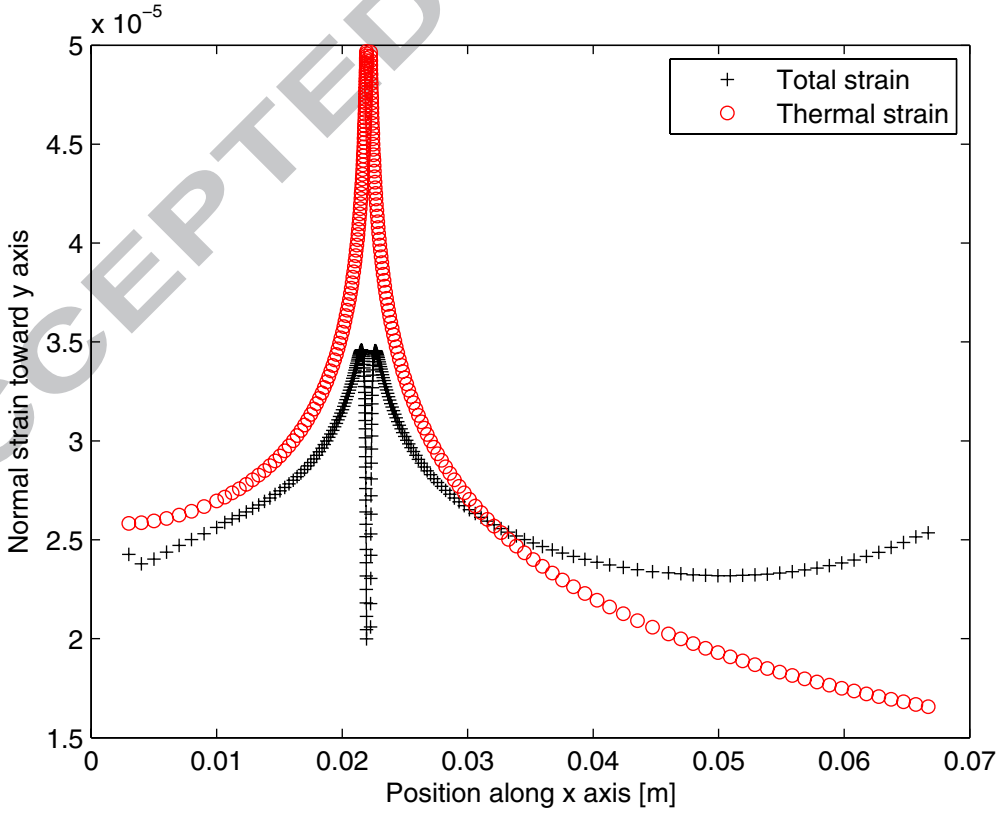

b)

Figure 12: Total and thermal normal strain distribution along x axis in the case of E4 test ($\Delta K = 20\,MPa\sqrt{m}$; $R = 0.1$): (a) normal strain toward x axis, (b) normal strain toward y axis.

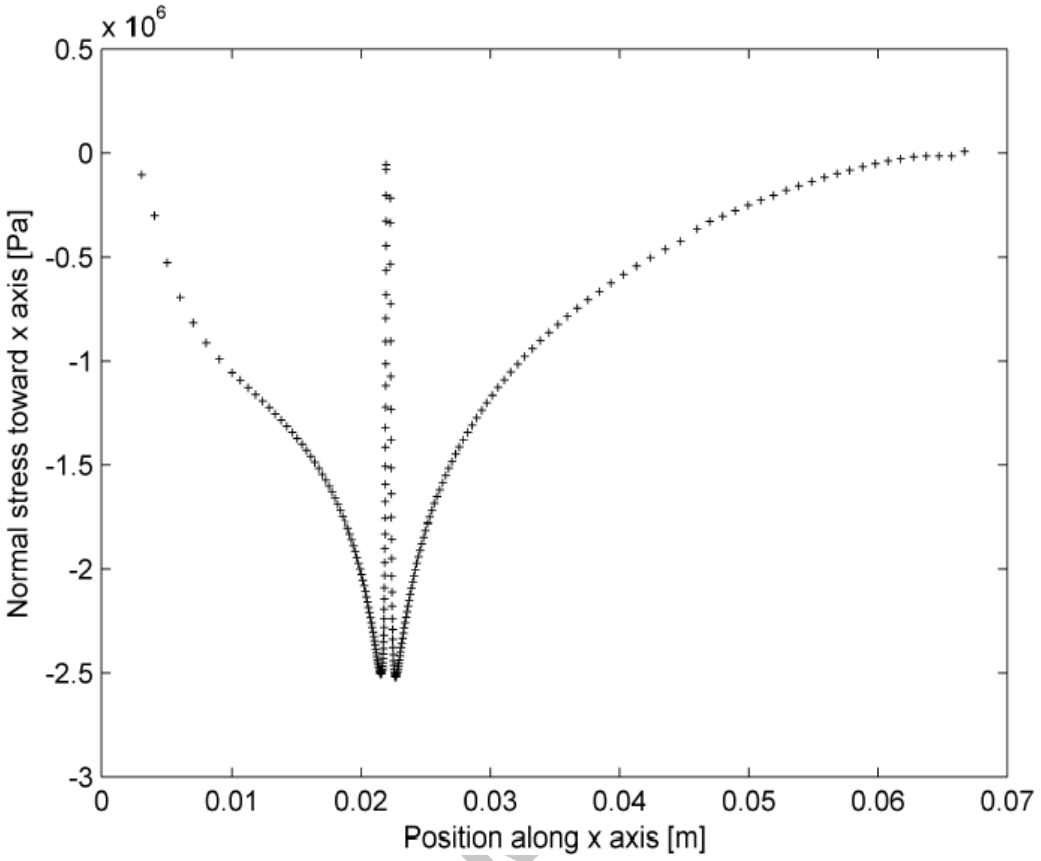

a)

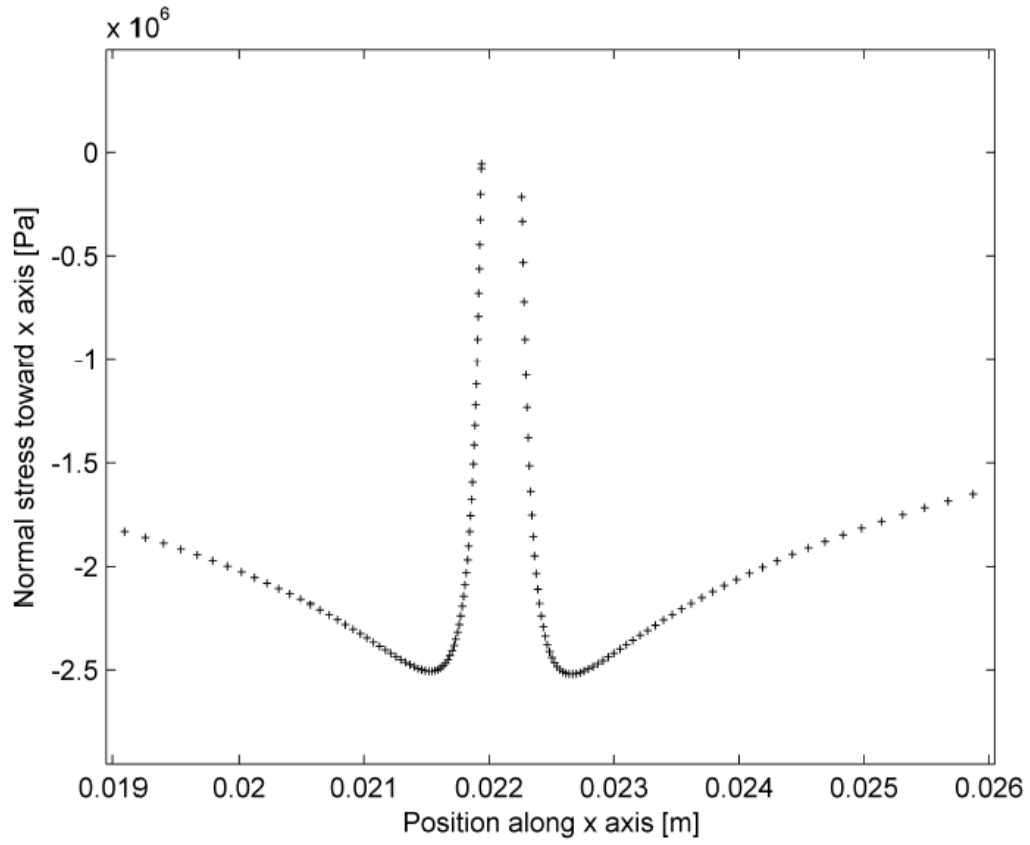

b)

Figure 13: Normal stress toward x axis distribution along x axis in the case of E4 test ($\Delta K = 20\,MPa\sqrt{m}$; $R = 0.1$): (a) general view, (b) enlargement near the reverse cyclic plastic zone.

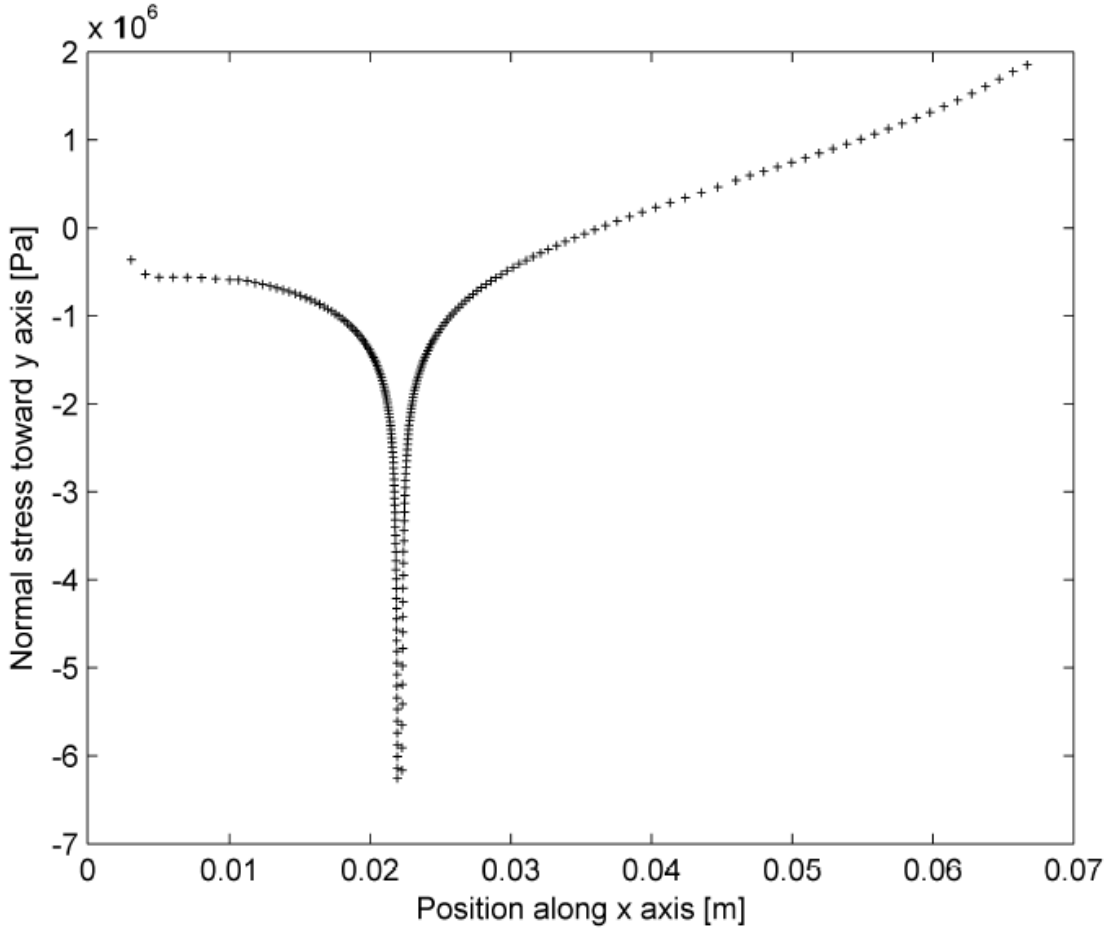

Figure 14: Normal stress toward y axis distribution along x axis in the case of E4 test ($\Delta K = 20\,MPa\sqrt{m}$; $R = 0.1$).